Energy dependence of two-nucleon transfer reactions on light nuclei

M. Pignanelli, S. Micheletti, I. Iori, P. Guazzoni, and F. G. Resmini
Istituto di Scienze Fisiche dell'Università di Milano, Italy,
and Istituto Nazionale di Fisica Nucleare, Sezione di Milano, Italy

J. L. Escudié
SPNME, Centre d'Etudes Nucléaires de Saclay, France
(Received 13 July 1973; revised manuscript received 27 February 1974)

The differential cross section has been measured at several incident proton energies between 20 and 45 MeV for the $^{14}N(p,^3He)^{12}C$, $^{15}N(p,t)^{13}N$, $^{15}N(p,^3He)^{13}C$, and $^{18}O(p,t)^{16}O$ reactions. Data on the energy dependence of other transfer reactions on the same nuclei, i.e., $^{18}O(p,d)^{17}O$, $^{14}N(p,\alpha)^{11}C$, and $^{18}O(p,\alpha)^{15}N$ reactions have also been obtained. These data are compared with distorted wave Born approximation (DWBA) predictions. The comparison indicates that the energy dependence of the cross sections is poorly explained by DWBA calculations based on single-step pickup which give a maximum in the cross section in the energy region where angular momentum matching conditions are achieved. The absence of corresponding maxima in the experimental excitation functions may indicate that other reaction mechanisms contribute substantially to the cross section. Theoretical approaches as successive pickup of the two nucleons and preequilibrium emission are also discussed.

[NUCLEAR REACTIONS $^{14}N(p,^3He)$, (p,α), $E=20.5$–44.6 MeV; measured $\sigma(E_{^3He},\theta)$; resolution 200 keV, $\theta_{lab}=12$–$166°$. Reaction mechanism analysis. $^{15}N(p,t)$, $(p,^3He)$, $E=24.0$–43.5 MeV; measured $\sigma(E_t,\theta)$, $\sigma(E_{^3He},\theta)$; resolution 200 keV, $\theta_{lab}=12$–$126°$. Enriched target. Reaction mechanism analysis. $^{18}O(p,d)$, (p,t), (p,α), $E=20.0$–43.6 MeV; measured $\sigma(E_d,\theta)$, $\sigma(E_t,\theta)$, $\sigma(E_\alpha,\theta)$; resolution 200 keV, $\theta_{lab}=14$–$164°$. Enriched target. Reaction mechanism analysis.]

I. INTRODUCTION

Two-nucleon transfer reactions have been studied in the past mainly to provide a test of the wave functions of the nuclear states involved[1-5] and have been usually regarded as proceeding through a direct single-step mechanism. Their analysis has been carried out in the framework of the distorted wave Born approximation (DWBA). Detailed investigations of the validity of this approach have been so far confined to one-nucleon transfer reactions on light and medium weight nuclei.[6-9] It is found that the method reliably describes direct surface reactions characterized by a high degree of localization in the angular momentum space.[10] This is usually the case of one-nucleon transfer reactions when low Q values and small transferred angular momenta are involved. Two-nucleon transfer reactions raise more difficulties, like the high sensitivity of the calculated cross sections to the choice of the heavy particle optical potential parameters and the evaluation of the two-particle form factors for the transferred nucleons. To reduce the uncertainties due to parameter ambiguities only relative values of the DWBA cross sections have usually been compared with the data. Most of the comparisons recently performed in the region of light nuclei have been limited to a single value of the incident energy.[2,4,5] The energy dependence has been explicity considered only in one case.[11]

The main purpose of this work is to investigate the reliability of the DWBA method when applied to the study of the energy dependence of two-nucleon transfer reactions on light nuclei. Differential cross sections of (p,t) and $(p,^3He)$ reactions have been measured at incident energies between 20 and 45 MeV on ^{14}N, ^{15}N, and ^{18}O and are reported in Sec. II. Data on other reactions like (p,d) or (p,α) on the same nuclei have also been taken.

The results of the comparison with the DWBA predictions are given in Sec. III. The poor overall agreement found for the cross sections energy dependence is discussed and the inadequacy of a standard DWBA description based on single-step pickup evidenced. A part of the discrepancies found could be attributed to contributions from two- or multi-step processes; different approaches have been recently formulated to treat these processes in two-nucleon transfer reactions. In Sec. IV the successive pickup of the two nucleons and the coupling of pickup and inelastic channels[12-14] are discussed. The energy dependences predicted by the precompound emission model[15,16] are compared to the data in Sec. V.

II. EXPERIMENTAL METHOD AND RESULTS

The measurements were performed with the 20 to 45 MeV proton beam of the Milan University AVF cyclotron. A gas target consisting of a 70 mm diameter cylindrical cell with entrance and exit windows of 2 mg/cm^2 Havar foils was used. The cell was run at a pressure of 0.5 atm using ^{14}N (natural nitrogen), 99.5% pure ^{15}N, and ^{18}O enriched to 98%. Two tantalum collimators were used to define the active volume of the gas as seen by the detectors. The front collimator was a 4 mm wide slit positioned at a distance of 44 mm from the center of the cell. The back collimator was circular, 4 mm in diameter, and located at 180 mm. The resulting angular spread was about ±1°. The emitted particles were detected by a ΔE-E telescope. The ΔE detectors were Si surface barrier junctions of 30 to 150 μm thickness; the E detectors were lithium-drifted Si junctions of 2 to 4 mm thickness. The detector thickness was selected according to the incident energy and the specific reaction studied. Mass identification was provided by the Ortec model 423 particle identifier. The over-all energy spread was of the order of 200 keV. Differential cross sections have been measured for the ^{18}O(p, t)^{16}O, ^{15}N(p, t)^{13}N, ^{15}N-(p, ^{3}He)^{13}C, and ^{14}N(p, ^{3}He)^{12}C reactions at several proton energies between 20 and 45 MeV and are shown in Figs. 1–3, 8, and 9. The levels observed are listed in Tables I–III together with their cross sections, integrated over the measured angular range. The energy dependence of the integrated cross sections is plotted in Fig. 11.

Data on the ^{18}O(p, d)^{17}O, ^{18}O(p, α)^{15}N, and ^{14}N-(p, α)^{11}C reactions have also been taken. The ^{15}N-(p, α)^{12}C data used in the analysis of Sec. V had been taken previously.[17] The observed deuteron angular distributions are shown in Fig. 4 and some differential cross sections for α particles at different incident energies are plotted in Fig. 5. The values of the integrated cross section for the transitions observed in the (p, d) reaction are shown in Fig. 11 and listed in Table IV; the corresponding data for the (p, α) reactions are shown in Fig. 14. Error bars, shown when significant, represent statistical errors only. The over-all normalization error is estimated to be within ±10%.

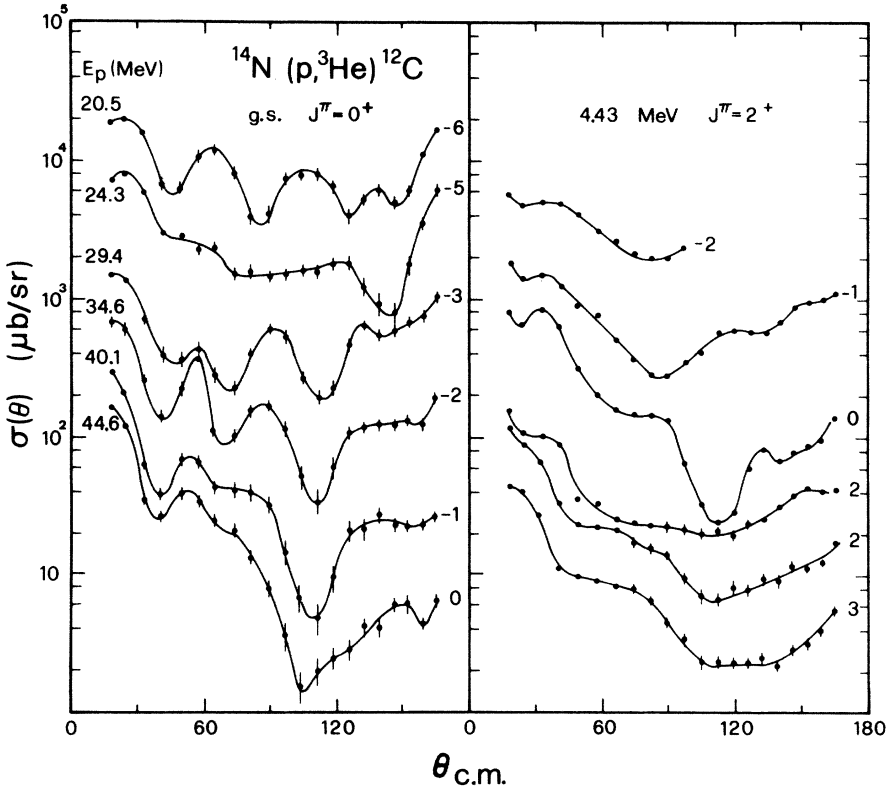

FIG. 1. Differential cross sections for the reaction ^{14}N(p, ^{3}He)^{12}C to the gound and 4.43 MeV states. Where not indicated, statistical errors are smaller than point size. The full lines are the result of a visual fit to the experimental points. The absolute cross section values are obtained as the product of the plotted cross sections time 2^n where n is the number given in the right side of the figure for each transition. Proton energies for the 4.43 MeV transition are the same and in the same order as for the ground state.

TABLE I. Integrated cross section of transitions to ^{16}O levels observed in the $^{16}O(p,t)^{18}O$ reaction.

Transition	Energy (MeV)	J^π	Integrated cross section[a] (mb) E_p =20.0 MeV	E_p =24.4 MeV	E_p =29.8 MeV	E_p =37.5 MeV	E_p =43.6 MeV
t_0	0.0	0^+	6.52	4.69	2.83	1.29	0.66
t_1+t_2	6.05+6.13	$0^+,3^-$	3.06	1.88	1.50	0.75	0.53
t_3+t_4	6.92+7.12	$2^+,1^-$	2.42	1.22	0.70	0.27	0.165
t_5	8.88	2^-	1.17	0.42	0.19	0.078	0.043
t_7	9.85	2^+	1.16	0.64	0.48	0.20	0.135
t_8	10.35	4^+	0.64	0.34	0.14	0.067	...

[a] Cross section integrated from 14 to 164° in the laboratory system.

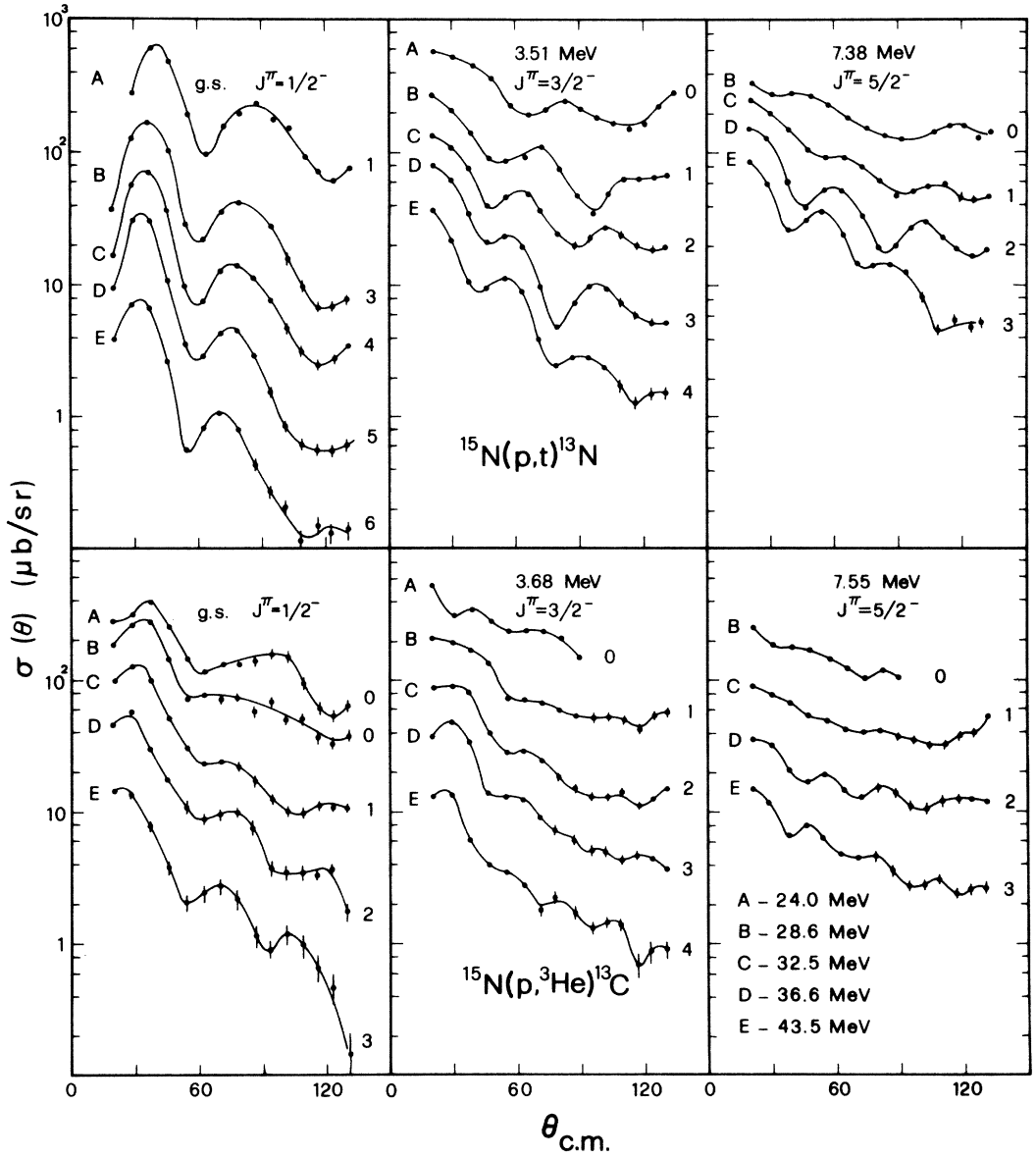

FIG. 2. Differential cross sections for the reactions $^{15}N(p,t)^{13}N$ and $^{15}N(p,\ ^3He)^{13}C$. See caption for Fig. 1.

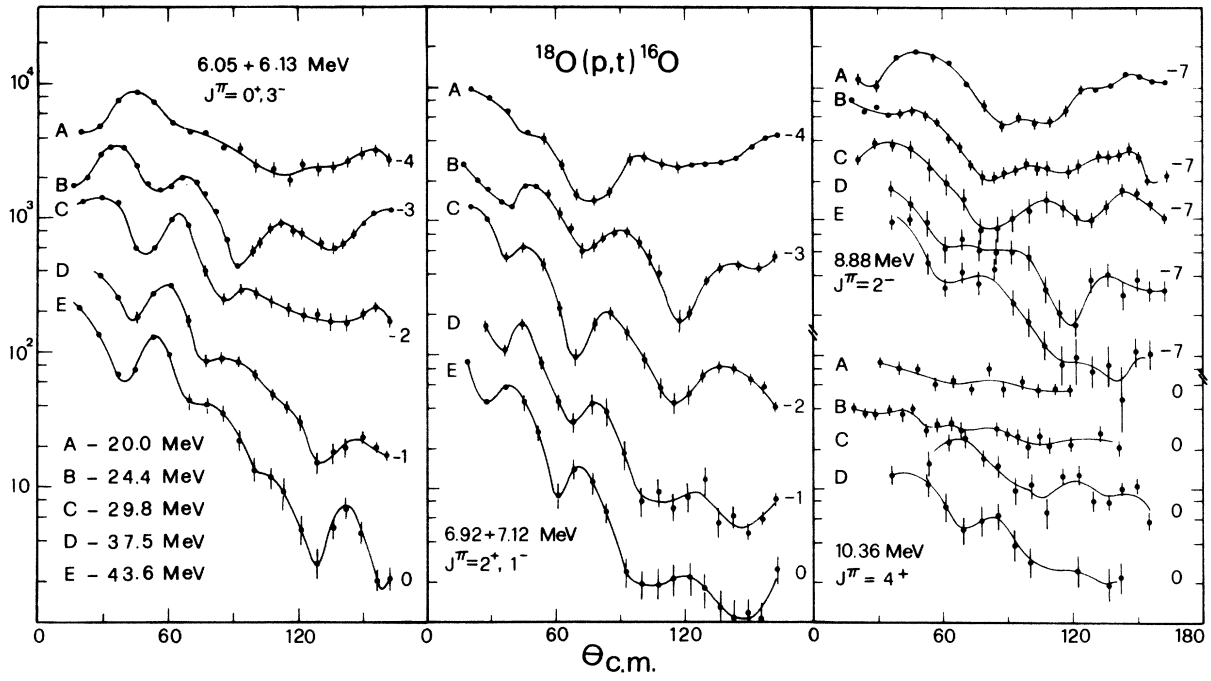

FIG. 3. Differential cross sections for the reaction $^{18}O(p, t)^{16}O$. See caption for Fig. 1.

III. DWBA ANALYSIS

A. Theory

The DWBA treatment of direct two-nucleon transfer reactions has been formulated by several authors[1, 18] in an essentially equivalent way. Following the formalism of Towner and Hardy[18] the expression for the differential cross section of the single-step, two-nucleon pickup reaction $A(a, b)B$ is:

$$\left(\frac{d\sigma}{d\Omega}\right)_{\text{pickup}} = \frac{\mu_a\mu_b}{(2\pi\hbar^2)^2}\frac{k_b}{k_a}\frac{1}{(2J_A+1)(2s_a+1)}\sum_{M_A M_B \sigma_a \sigma_b}|T_{fi}|^2$$

$$= \frac{\mu_a\mu_b}{(2\pi\hbar^2)^2}\frac{k_b}{k_a}\frac{2s_b+1}{2s_a+1}$$

$$\times\sum_{M\sigma_a\sigma_b}^{J}\left|\sum^{[n_1l_1j_1][n_2l_2j_2]LSJ} b_{ST}S_{AB}{}^{1/2}([n_1l_1j_1][n_2l_2j_2];JT)(T_BN_BTN \mid T_AN_A)\begin{bmatrix} l_1 & l_2 & L \\ \frac{1}{2} & \frac{1}{2} & S \\ j_1 & j_2 & J \end{bmatrix}\circledast^{LSJT}_{M\sigma_a\sigma_b}\right|^2, \quad (1)$$

TABLE II. Integrated cross section of transitions to ^{13}N and ^{13}C levels observed in the $^{15}N(p,t)^{13}N$ and $^{15}N(p,{}^3He)^{13}C$ reactions.

Transition	Energy (MeV)	J^π	Integrated cross section[a] (mb) E_p = 24.0 MeV	E_p = 28.6 MeV	E_p = 32.5 MeV	E_p = 36.6 MeV	E_p = 43.5 MeV
t_0	0.0	$\frac{1}{2}^-$	4.05	3.60	2.66	2.03	0.88
t_1[b]	3.51	$\frac{3}{2}^-$	2.76	1.89	1.64	1.39	0.95
t_2	7.38	$\frac{5}{2}^-$	...	1.87	1.68	1.64	1.61
h_0	0.0	$\frac{1}{2}^-$	1.60	0.94	0.66	0.50	0.25
h_1[b]	3.68	$\frac{3}{2}^-$	2.26	1.63	1.21	0.98	0.51
h_2	7.55	$\frac{5}{2}^-$	...	1.45	0.98	0.66	0.40

[a] Cross section integrated from 12 to 126° in the laboratory system.

[b] This transition corresponds to a doublet. The level indicated has however been found (Ref. 4) to give a dominant contribution.

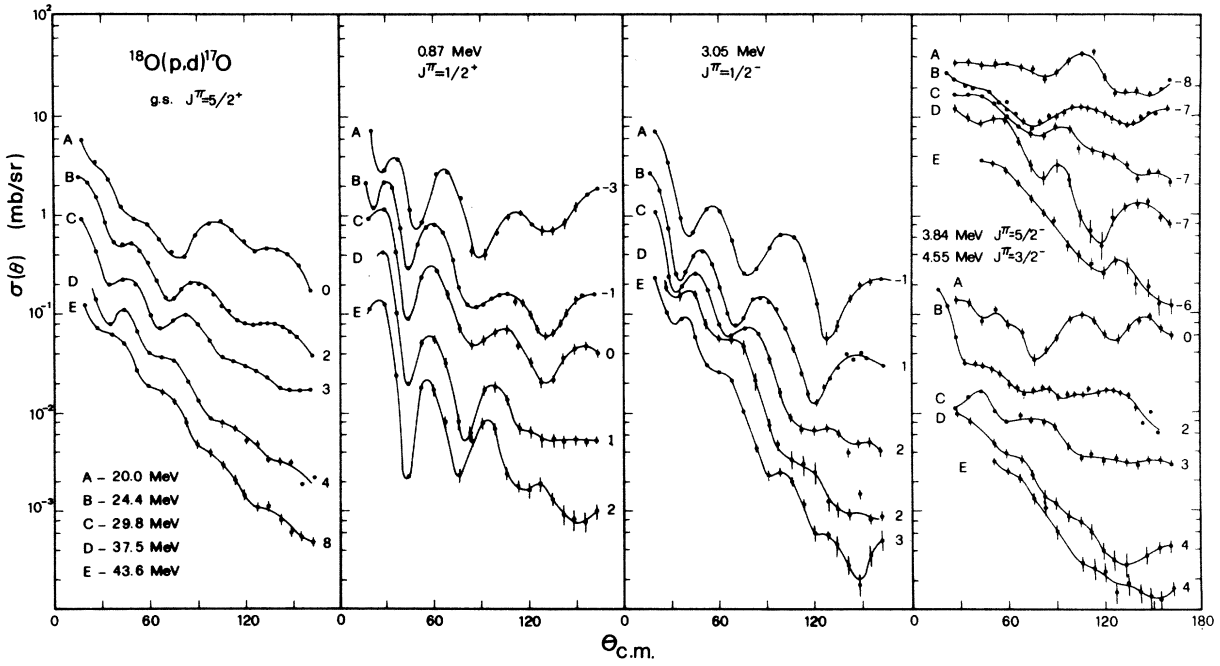

FIG. 4. Differential cross sections for the reaction $^{18}O(p, d)^{17}O$. See caption for Fig. 1.

where $[n_1 l_1 j_1]$ and $[n_2 l_2 j_2]$ are the quantum numbers defining the single particle states of the two transferred nucleons and L, S, J, and T are the quantum numbers of the transferred pair. All the nuclear structure information is contained in the spectroscopic amplitude $S_{AB}{}^{1/2}$; the factor $b_{ST}{}^2$ is essentially a spectroscopic factor for the light particle. The term $\mathcal{B}_{M\sigma_a\sigma_b}^{LSJT}$ contains the details of the integration of the radial wave function and depends upon the character of the two-body force. The different two-nucleon configurations are added coherently so that the spectroscopic amplitudes cannot be factored out.

The code DWUCK and the DWBA two-nucleon transfer code of Nelson and Macefield[19] have been used. The latter allows one to perform coherent sums over S and L values and to choose between several methods for the calculation of the bound state wave function of the transferred pair. This is, in the Rook-Mitra approach, a product of two Woods-Saxon wave functions each one describing a nucleon bound with an energy one half the total experimental binding energy for the pair. Other methods use harmonic oscillator wave functions for the internal and center of mass motion of the transferred pair or retain Woods-Saxon wave functions expanded in terms of harmonic oscillator wave functions. Details and advantages of the different methods are discussed by Nelson, Chant, and Fisher.[20] For the bound state well a radius $R=1.25A^{1/3}$ fm and a diffuseness $a=0.65$ fm were used. The spin-orbit term was taken 25 times larger than the Thomas value. The spectroscopic amplitudes used for the cross section calculations are those given by Cohen and Kurath[21] for the reactions on ^{14,15}N and by Zuker[22] for the reaction on ^{18}O.

B. Optical model parameters

In the DWBA analysis of transfer reactions it is customary to assume that the optical model parameters to be used are those determined from elastic scattering.

TABLE III. Integrated cross section of transitions to ^{12}C levels observed in the ^{14}N(p,^{3}He)^{12}C reaction.

Transition	Energy (MeV)	J^π	Integrated cross section[a] (mb) E_p =20.5 MeV	E_p =24.3 MeV	E_p =29.4 MeV	E_p 34.6 MeV	E_p =40.1 MeV	E_p =44.6 MeV
h_0	0.0	0^+	1.59	0.92	0.78	0.48	0.25	0.21
h_1	4.43	2^+	9.60	4.20	3.30	2.30	1.02	0.83

[a] Cross section integrated from 12 to 166° in the laboratory system.

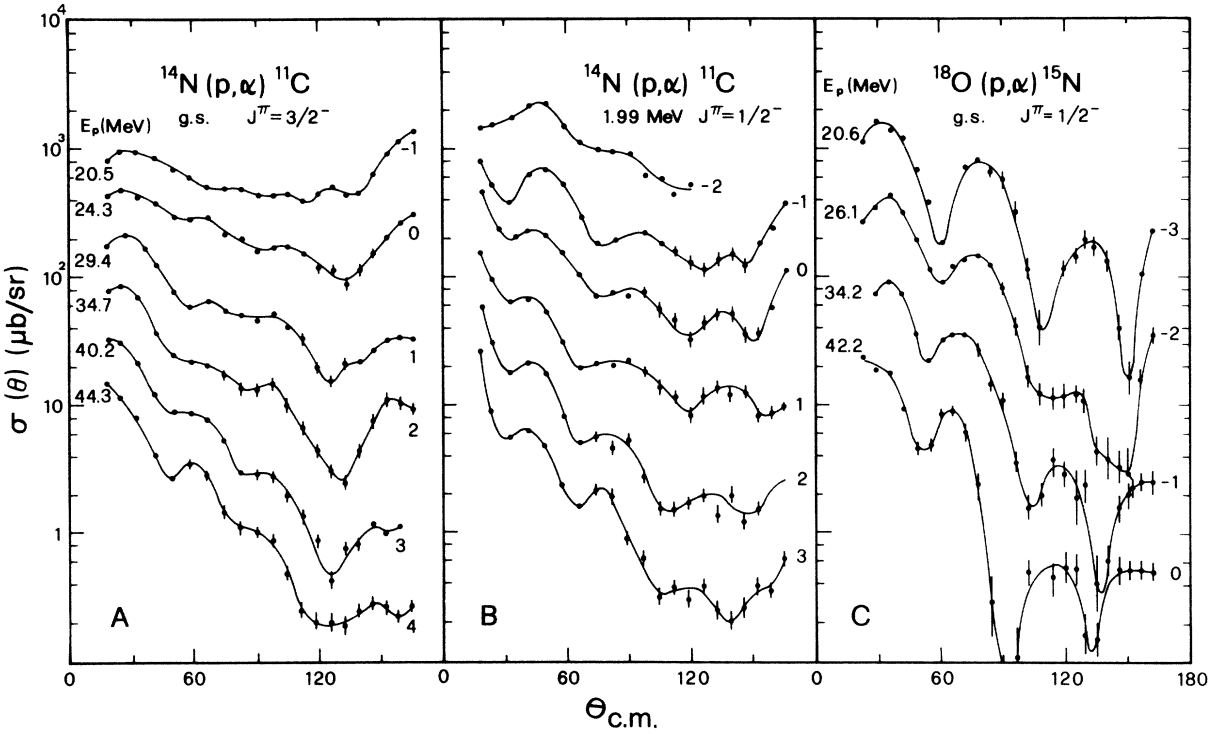

FIG. 5. Differential cross sections for the reaction ^{14}N(p, α)^{11}C to the ground state [part (a)] and to the 1.99 MeV level [part (b)]. In part (c) is plotted the differential cross section for the reaction ^{18}O(p, α)^{15}N to the ground state of ^{15}N. See caption for Fig. 1.

Proton optical parameters have been obtained from an analysis, performed with the code MERCY,[23] of the existing proton elastic scattering data, for the nuclei concerned, over the energy range of interest. These potentials and the energies at which have been taken the experimental data considered are listed in Table V. Figure 6 shows the fits to the proton elastic scattering data on ^{14}N, ^{15}N, and ^{18}O given, respectively, by potentials $P1$, $P3$, and $P7$. Average potentials have been given by several authors: acceptable fits to the elastic scattering data are obtained using the potential given by Watson, Singh, and Segel[24] for ^{14,15}N and by Menet *et al.*[25] for ^{18}O. These potentials are also reported in Table V as sets $P2$, $P5$, and $P9$, respectively.

Few triton elastic scattering experiments have been performed and consequently only the potential by Glover and Jones[26] for triton elastic scattering on ^{16}O at 12 MeV, labeled as $T1$, is available for the nuclei of interest in the energy range 10–30 MeV. It has been shown,[27] however, that triton potentials with geometries similar to that of $T1$ give acceptable fits over a wide energy range. As customary, owing to the paucity of triton scattering data, helion (^{3}He) optical potentials have been used also for the triton channels. When the analysis of helion elastic scattering is attempted additional difficulties are encountered because of the well known existence of a multiplicity of solutions. Optical

TABLE IV. Integrated cross section of transitions to ^{17}O levels observed in the ^{18}O(p,d)^{17}O reaction.

Transition	Energy (MeV)	J^π	Integrated cross section[a] (mb) E_p = 20.0 MeV	E_p = 24.4 MeV	E_p = 29.8 MeV	E_p = 37.5 MeV	E_p = 43.6 MeV
d_0	0.0	$\frac{5}{2}^+$	11.20	13.19	10.94	6.87	6.36
d_1	0.87	$\frac{1}{2}^+$	2.15	2.11	1.48	0.99	0.58
d_2	3.058	$\frac{1}{2}^-$	4.36	4.24	4.18	2.25	2.07
d_3	3.85	$\frac{5}{2}^-$	1.33	1.19	0.66	0.35	0.26
d_4	4.55	$\frac{3}{2}^-$	0.88	0.83	0.63	0.43	0.28

[a] Cross section integrated from 14 to 164° in lab system.

TABLE V. Proton optical model parameters. The potential has the form:

$$V(r) = V_C(r) - Vf_V(r) - iWf_W(r) + 4ia_W W_D f'_D(r) - \left(\frac{\hbar}{Mc}\right)^2 V_{so} \frac{1}{r} f'_{so}(r)\,\vec{\sigma}\cdot\vec{l}$$

with

$$f_X = (1 + e^{(r - r_X A^{1/3})/a_X})^{-1}$$

and V_C is the Coulomb potential due to a uniformly charged sphere of radius $r_C A^{1/3}$ with $r_C = 1.25$ fm. Energy dependent terms are set equal to zero when they result negative. The χ^2 values reported correspond to a 10% error in the experimental points.

Nucleus and set	Particle energy (MeV)	V	W	W_D	V_{so}	r_V	a_V	r_W	a_W	r_{so}	a_{so}	χ^2
^{14}N-P1	18,[a]21,[b]24,[c]26 [a] 31,[d]49.4 [e]	$61 - 0.35E$	$0.17E - 5.1$	$6.1 - 0.035E$	5.65	1.11	0.644	1.36	0.52	1.0	0.53	4.2
^{14}N-P2	Ref. 24	$60.66 - 0.28E$	f	g	5.5	$1.15 - 0.001E$	0.57	As r_V	0.5	As r_V	0.57	7.8
^{15}N-P3	22.4,[h]24.5,[h]26 [h] 39.84 [i]	$57.6 - 0.2E$	$0.23E - 6.9$	$6.9 - 0.07E$	4.7	1.05	0.72	1.47	0.48	0.71	0.69	3.0
^{15}N-P4	As P3	$48.0 - 0.2E$	$0.36E - 10.7$	$6.6 - 0.095E$	4.8	1.2	0.61	1.38	0.6	1.0	0.74	4.0
^{15}N-P5	Ref. 24	$64.2 - 0.28E$	f	g	5.5	$1.15 - 0.001E$	0.57	As r_V	0.5	As r_V	0.57	
^{15}N-P6	Adjusted from P5	52.5	f	g	5.5	$1.15 - 0.001E$	0.57	As r_V	0.5	As r_V	0.57	
^{18}O-P7	13.04,[j]16.28,[j]22.5 [k] 24.5,[k]29.8,[k]66.5 [l]	$57.6 - 0.2E$	$0.15E - 4.5$	$7.2 - 0.06E$	4.9	1.07	0.74	1.34	0.64	0.9	0.57	2.1
^{18}O-P8	As P7	$52.1 - 0.21$	$0.36E - 10.7$	$7.42 - 0.067E$	5.1	1.16	0.66	1.29	0.65	1.0	0.62	5.9
^{18}O-P9	Ref. 25	$56.0 - 0.22E$	$1.2 + 0.09E$	$5.92 - 0.05E$	6.04	1.16	0.75	1.37	$0.85 - 0.008E$	1.064	0.78	
^{18}O-P10	Ref. 50	$57.9 - 0.32E$	$0.22E - 2.7$	$1.13 - 0.25E$	6.2	1.17	0.75	1.32	0.588	1.01	0.75	
^{18}O-P11	Adjusted from P10	56.0	As P10	As P10	6.2	1.17	0.75	1.32	0.588	1.01	0.75	

[a] H. F. Lutz, D. W. Heikkinen, and W. Bartolini, Nucl. Phys. A198, 257 (1972).
[b] N. Baron, R. F. Leonard, and D. A. Lind, Phys. Rev. 180, 978 (1969).
[c] J. L. Escudié, A. Tarrats, Compte rendu d'activité 1969/70, note No. CEA-N 1390 (unpublished), p. 96.
[d] C. C. Kim, S. M. Bunch, D. W. Devins, and H. H. Forster, Nucl. Phys. 58, 32 (1964).
[e] N. M. Clarke, E. J. Burge, D. A. Smith, and J. C. Dore, Nucl. Phys. A157, 145 (1970).
[f] $W = 0$ for $E < 35$ MeV; $W = (E - 35) \times 1.07$ for $35 < E < 42$ MeV; $W = 7.5$ for $E > 42$ MeV.
[g] $0.60E$ for $E < 14.7$ MeV; $9.6 - 0.056E$ for $E > 14.7$ MeV.
[h] J. L. Escudié, R. M. Lombard, M. Pignanelli, F. Resmini, and A. Tarrats, Compte rendu d'activité, note No. CEA-N 1522 (unpublished), p. 123.
[i] J. L. Snelgrove and E. Kashy, Phys. Rev. 187, 1259 (1969).
[j] J. Stevens, H. F. Lutz, and S. F. Eccles, Nucl. Phys. 70, 129 (1969).
[k] F. Resmini, R. M. Lombard, M. Pignanelli, J. L. Escudié, and A. Tarrats, Phys. Lett. 37B, 275 (1971).
[l] G. M. Lerner and J. B. Marion, Nucl. Phys. A193, 593 (1972).

parameters have been obtained with the only constraint that the real well depth should be about three times that for protons with a reasonable geometry. Some of the sets so derived are given in Table VI labeled as $H1$, $H2$, and $H7$. Del Vecchio and Daehnick[28] have suggested to use in a transfer reaction the same real well geometries for all the potentials generating scattered and bound state wave functions. Imposing this further restriction the sets $P4$, $P8$, $H3$ and $H6$ were obtained. The energy independent set of Hiebert, Newman, and Bassel[29] for 29 MeV helions elastic scattering on ^{14}N, widely used in the analysis of reactions on light nuclei, has also been used and is listed in Table VI as $H4$. Some fits are shown in Fig. 7.

Another approach attempted[2,4,11] in two-nucleon transfer reaction analysis is to choose, within reasonable limits, the parameters so as to obtain a good fit to the transitions considered. We have found it profitable to use the sets $P5$, $H4$ and $P10$, $T1$, respectively, for reactions on ^{14,15}N and ^{18}O as starting points for this procedure. The "adjusted" potentials so obtained are those labeled $P6$, $P11$ for protons and $H5$, $T2$ for mass-3 particles. It is remarkable that these proton potentials do not require an energy dependence for the real well depth, as also found by Van Oers and Cameron[30] for scattering on ^{16}O in the 20–40 MeV energy interval. Also potentials $P3$ and $P7$ present a weak energy dependence.

C. Comparison with DWBA single-step pickup calculations

Typical DWBA fits are shown in the Figs. 8 and 9. The shape of the differential cross sections is not well reproduced using the potentials here derived from the elastic scattering also following the

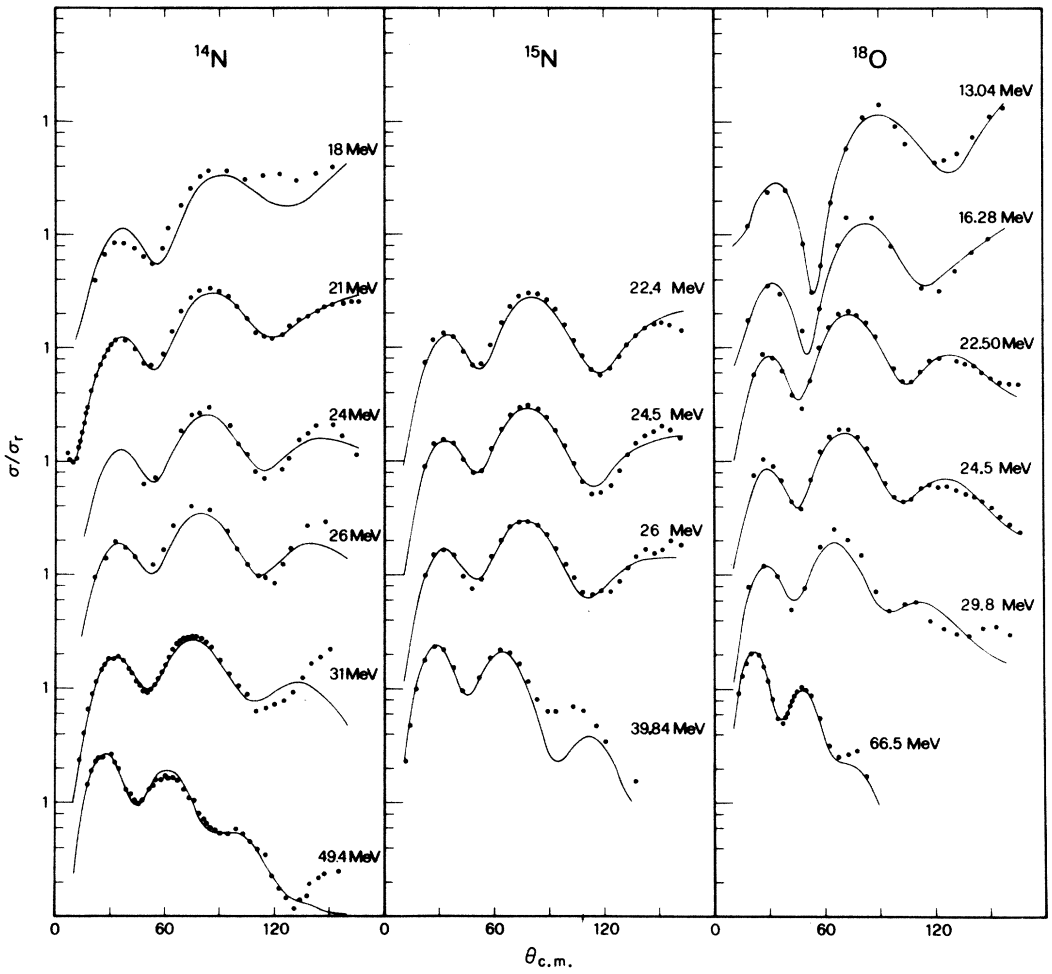

FIG. 6. Differential cross sections for proton elastic scattering (relative to the Rutherford cross section). The curves represent optical model fits calculated with the potentials $P1$, $P3$, and $P7$ of Table V.

TABLE VI. Mass-three particle optical potentials. See caption of Table V for the potential form.

Nucleus and set	Particle energy (MeV)	V	W	W_D	V_{so}	r_V	a_V	r_W	a_W	r_{so}	a_{so}	χ^2
^{12}C-$H1$	11,[a] 15,[a] 18.6,[b] 20,[b] 23.9 [b] 28.95,[c] 34.7,[d] 39.6,[d] 42 [e]	$150-0.594E$	$0.5E$ $(E<22)$ $14.6-0.0975E$	···	4.0	1.1	0.715	1.83	0.97	1.1	0.715	15.64
^{13}C-$H2$	12,[f] 15,[f] 18,[f] 20 [g] 35.7,[h] 39.6 [i]	$173-0.2E$	$12.5+0.09E$		2.5	1.3	0.6	1.67	0.88	1.3	0.6	16.9
^{13}C-$H3$	As $H2$	$196-0.425E$	···	$12.7+0.0725E$	···	1.2	0.61	1.166	0.86	···	···	13.6
^{13}C-$H4$	Ref. 29	196	32.1	···	···	1.14	0.675	1.82	0.56	···	···	···
^{13}C-$H5$	Adjusted from $H4$	$169-0.2E$	$6.5+0.177E$	···	···	1.14	0.5	1.82	0.56	···	···	···
^{16}O-$H6$	10.31,[j] 16.6,[k] 25.8,[k] 36.6 [k]	$162+0.474E$	$8.6+0.064E$	···	7.0	1.16	0.66	1.9	0.8	1.16	0.66	10.36
^{16}O-$H7$	As $H6$	131	19.6	···	···	1.46	0.5	1.43	1.0	···	···	11.27
^{16}O-$T1$	Ref. 26	146.8	18.4	···	···	1.4	0.551	1.4	0.551	···	···	···
^{16}O-$T2$	Adjusted from $T1$	146.8	$7.5+0.4E$	···	···	1.4	0.44	1.4	0.551	···	···	···

[a] G. Scheklinski, U. Strohbusch, and B. Goel, Nucl. Phys. A153, 97 (1970); R. W. Zurmühle and C. M. Fou, *ibid.* A129, 502 (1969).
[b] S. I. Warshaw, A. J. Buffa, J. B. Barengoltz, and M. K. Brussel, Nucl. Phys. A121, 350 (1968).
[c] D. J. Baugh, G. J. B. Pyle, P. M. Rolph, and S. M. Scarrott, Nucl. Phys. A95, 115 (1967).
[d] T. Fujisawa, S. Yamaji, K. Matsuda, S. Motonaga, F. Yoshida, H. Sakaguchi, and K. Masui, J. Phys. Soc. Jap. 34, 5 (1973).
[e] R. N. Singh, N. De Takacsy, S. I. Hayakawa, R. L. Hutson, and J. J. Kraushaar, Nucl. Phys. A205, 97 (1973).
[f] E. M. Kellog and R. W. Zurmühle, Phys. Rev. 152, 890 (1966).
[g] J. L. Escudié, M. Pignanelli, F. Reɜmini, and Y. Terrien, private communication.
[h] K. P. Artemov, V. Z. Goldberg, and V. P. Rudakov, Yad. Fiz. 9, 1173 (1969) [transl.: Sov. J. Nucl. Phys. 9, 686 (1969)].
[i] G. C. Ball and J. Cerny, Phys. Rev. 177, 1466 (1969).
[j] K. H. Bray and J. Nurzynski, Nucl. Phys. A127, 622 (1969).
[k] K. P. Artemov, V. Z. Goldberg, B. I. Islamov, V. P. Rudakov, and I. N. Serikov, Yad. Fiz. 1, 629 (1965) [transl.: Sov. J. Nucl. Phys. 1, 450 (1965)].

geometrical prescriptions of Del Vecchio and Daenick.[28]

In the attempt to improve the fits it was found that the most critical choice was that of mass-3 potentials. Better fits were obtained using energy independent potentials such as $H4$ and $T2$ for mass-3 particles. In this case proton potentials derived from elastic scattering and average sets are equivalent. The position of maxima and minima is reproduced over the entire energy range for $L=0$ transitions and at least at some energies for $L\neq 0$ transitions. Satisfactory fits are obtained over the entire energy range for all transitions only by "adjusting *ad hoc*" the optical model potentials.

The comparison between the experimental and the calculated values of the differential cross sections at the position of the first measured maximum, as a function of the incident energy, is however generally unsatisfactory also when these "adjusted" potentials are used, as shown in Fig. 10 for three transitions chosen as typical examples. Similar results are obtained if one considers the (p, t) and $(p, {}^3\mathrm{He})$ cross sections integrated over all the experimental angular range, as shown in Fig. 11. A satisfactory agreement is found only for the two (p, t) ground state transitions both corresponding to $L=0$ transfers, but it greatly deteriorates for the other (p, t) and $(p, {}^3\mathrm{He})$ transitions. It is worth noticing that the slopes of the experimental curves often resemble each other more than the calculated ones.

D. Kinematical aspects

In order to understand some features of the calculated curves, we shall discuss the effects produced by the parameters and the assumptions entering DWBA calculations. In Fig. 12 we report, as an example, the tests performed for the transi-

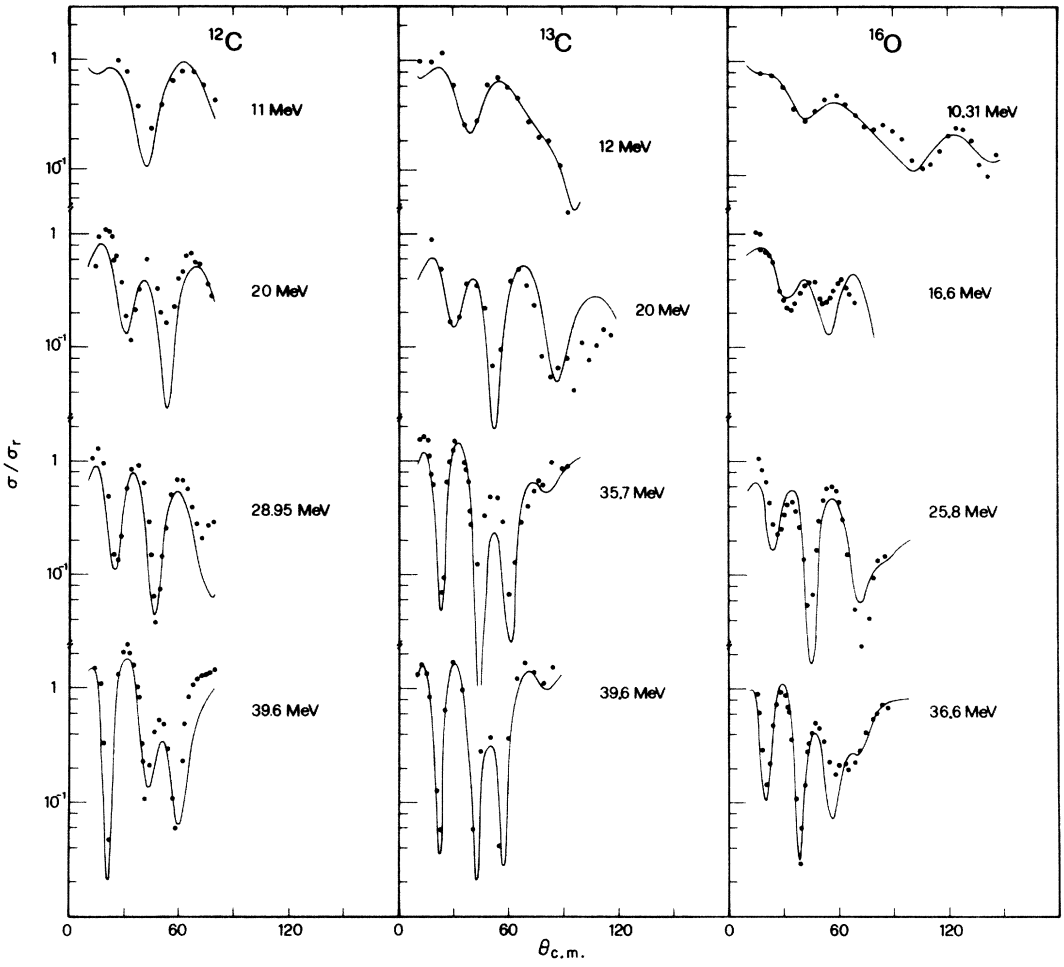

FIG. 7. Differential cross sections for helion elastic scattering (relative to the Rutherford cross section). The curves represent optical model fits obtained using the potentials $H1$, $H3$, and $H6$ of Table VI.

tions to the ground state (g.s.) and to the 2^+ state at 9.85 MeV in ^{16}O which correspond to $L=0$, $Q=-3.7$ MeV and $L=2$, $Q=-13.7$ MeV, respectively.

In part (a) of Fig. 12 some curves calculated using different optical model parameters are shown. It is evident that, while the calculated curves depend upon the parameters used, the choice of any particular set does not alter substantially the energy dependence which is obtained, in contrast with the widely varying quality obtained for the fits to the angular distributions.

In part (b) of the same figure are shown the results obtained with the methods for the calculation of the form factor listed in Sec. III A and by using the potentials $P11$ and $T2$. Other potentials give equivalent results. Once more the energy dependence is not substantially altered and remains characteristic of the Q and L values.

The effect on the calculations of the zero-range approximation has also been investigated. Different approaches[31-33] have been proposed to evaluate finite-range corrections. Recently an exact calculation, in which all transferred nucleons are assumed grouped in a cluster, has been reported by Perrenoud and Devries.[34] Tests have been performed both using the approximate procedure of Bencze and Zimanyi[31] included in the Nelson-Macefield code and the method of Perrenoud and Devries using the DWUCK code as modified by Devries.[35] The results obtained for the energy dependence are given in part (b) of Fig. 12 as FR-BZ and FR-DP, respectively. Although sizeable alterations are introduced in the energy dependence, the agreement with the data is not improved and the general trend remains again characteristic of the Q and L values.

Large effects are instead produced, as shown in part (c) of Fig. 12, by changing the Q value, either using a fixed binding energy for the transferred particles or employing the more often used prescription $E_B=(S_{nn}-E_{exc})/2$ where S_{nn} and E_{exc} are, respectively, the experimental g.s. separation energy of the transferred group and the excitation

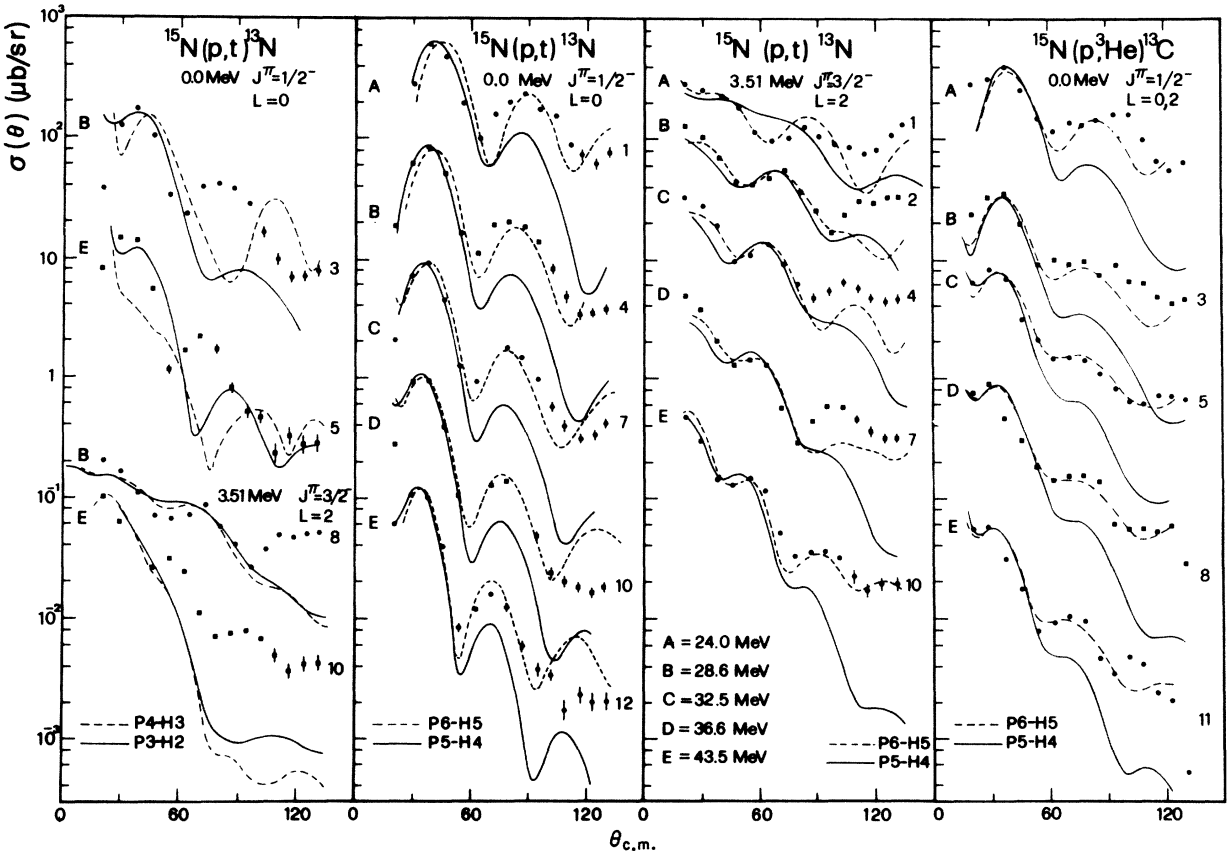

FIG. 8. Comparison of reaction cross sections with DWBA calculations. Typical fits obtained with potentials derived from elastic scattering in the present work are given in the left part; the other parts show the fits obtained with the average set $P5$ and energy independent set $H4$ and with the "adjusted potentials" $P6$ and $H5$. The comma between two values of the transferred angular momentum L indicates coherent sum. See caption of Fig. 1 for other details.

energy of the final state in the residual nucleus. From part (c) of Fig. 12 it is apparent that an uniformly decreasing curve, similar to the experimental ones (Fig. 11), is obtained in the energy interval between 20 and 45 MeV only for low L and small negative Q values. For larger values of these quantities the calculated cross sections show a broad maximum.

Since such a behavior can hardly be attributed, because of the above arguments, to an unfortunate choice of the parameters or to details of the calculations, it should be regarded as intrinsic to the kinematical description of the reaction as given by standard single-step DWBA. One can indeed demonstrate that a maximum in the calculated cross sections appears at the incident energy for which the conditions of best matching on angular momenta are achieved.

Besides the kinematical factor k_b/k_a, the energy dependence of the calculated cross section is determined by the square of the quantity $\mathcal{B}^{LSTJ}_{\sigma_a\sigma_b}$ which contains another kinematical factor $1/(k_a k_b)^2$ and the square of the radial integrals. These are dominated by the overlap of the incoming and outgoing distorted waves.[10] The maximum overlap is obtained when the following conditions are verified: (i) the momenta k_a and k_b have comparable values; (ii) the first maxima in the wave functions of the incoming and outgoing channels coincide. In our case $k_t(k_{^3\mathrm{He}})$ and k_p are never very different and, for many transitions, are equal at proton energies around 30 MeV. The second condition is verified when angular momentum matching conditions are achieved. This requires $L_a/k_a \simeq L_b/k_b$, with $L_a - L_b = L$, where L is the transferred angular momentum, and L_a and L_b are the angular momenta for the incoming and outgoing partial waves for which the transmission coefficient $|T_L|$

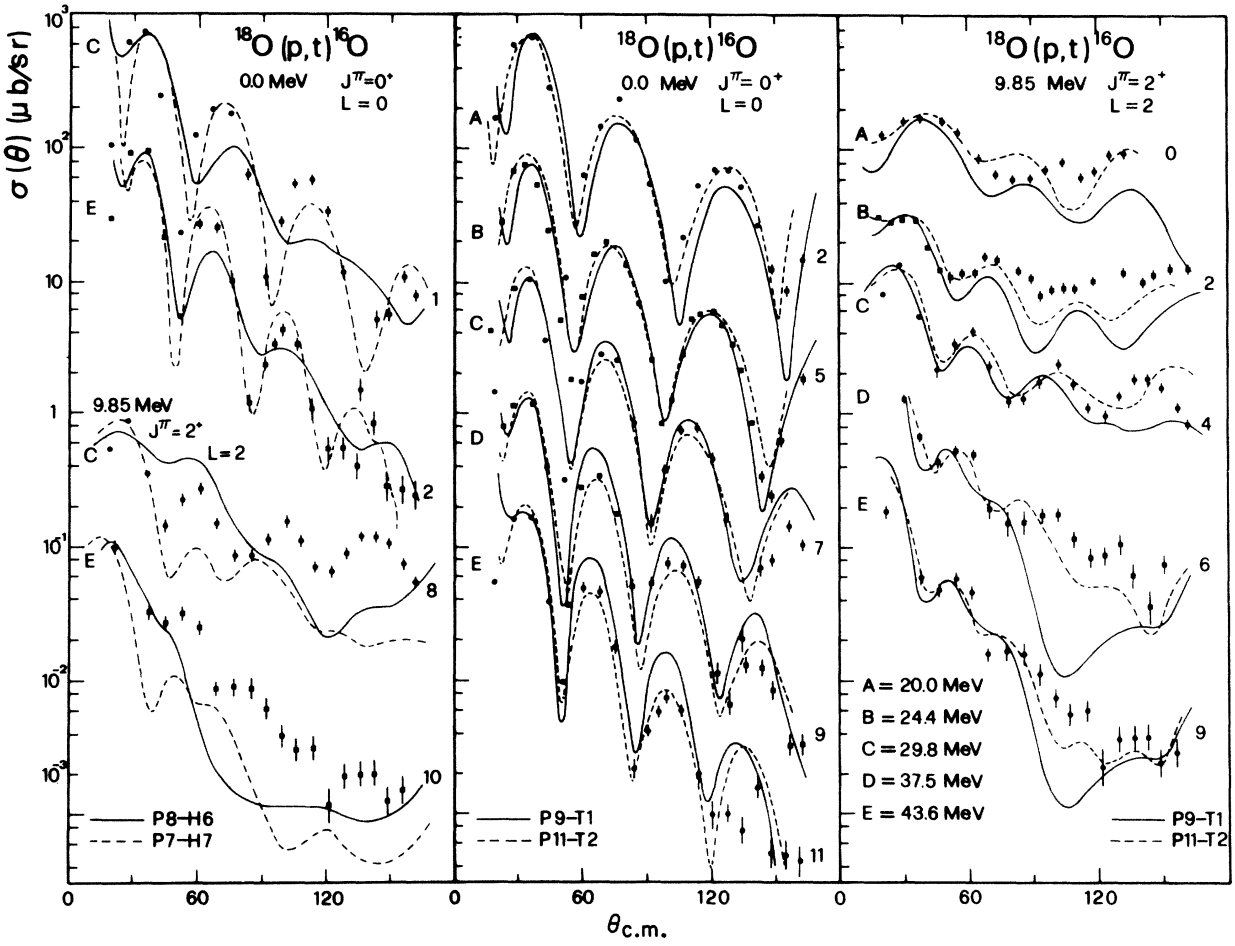

FIG. 9. Comparison of reaction cross sections with DWBA calculations. Typical fits obtained with potentials derived from elastic scattering in the present work are given in the left part; the other parts show the fits obtained with the average set $P9$ and energy independent set $T1$ and with the "adjusted potentials" $P11$ and $T2$. See caption of Fig. 1 for other details.

is about $\frac{1}{2}$. The partial waves in the region around L_a and L_b give indeed the largest contributions to the reaction. Typical transmission coefficient curves for two Q values and for several incident energies are reported in Fig. 13(a). In our energy range the angular momentum matching conditions for $L=0$ are never fulfilled for the Q value corresponding to the ground state transition; they are reached at 20 MeV only for $Q=-13.7$ MeV. The resulting radial integrals, shown in Fig. 13(b), increase slowly and uniformly with proton energy for $Q=-3.7$ MeV. The product of the complete kinematical factor $1/k_a\,{}^3k_b$ and of the square of the radial integrals results in a cross section uniformly decreasing with proton energy. For $L=2$ and $k_t \simeq k_p$ matching conditions are achieved for $L_t - L_p = 2$. From Fig. 13(a) we see that these are fulfilled at about 30 MeV for $Q=-13.7$ MeV. The resulting radial integrals, which are given in Fig. 13(b), show the largest relative increase and a good L localization around 30 MeV: this effect combined with the uniform decrease of the kinematical factor results in a maximum in the cross section around 30 MeV.

From the above arguments it is apparent that the kinematical features of two-nucleon transfer reactions as described by the DWBA formalism, lead to a maximum in the energy dependence of the calculated cross sections, and that such a be-

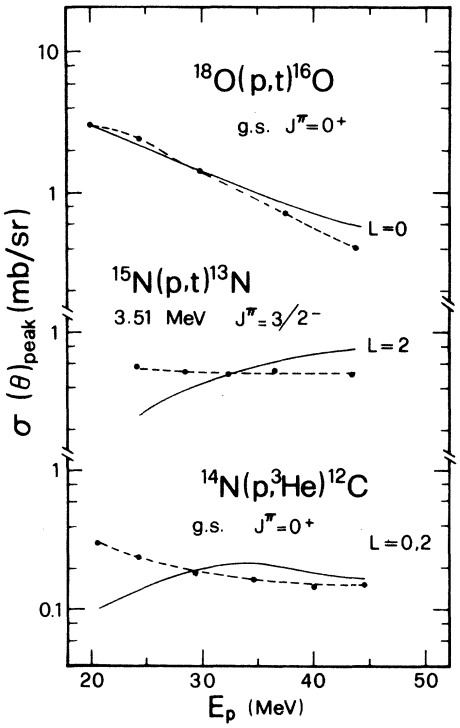

FIG. 10. Comparison between first maximum peak cross sections values (points and dashed curves) and arbitrarily normalized DWBA predictions (full curves) as a function of incident energy.

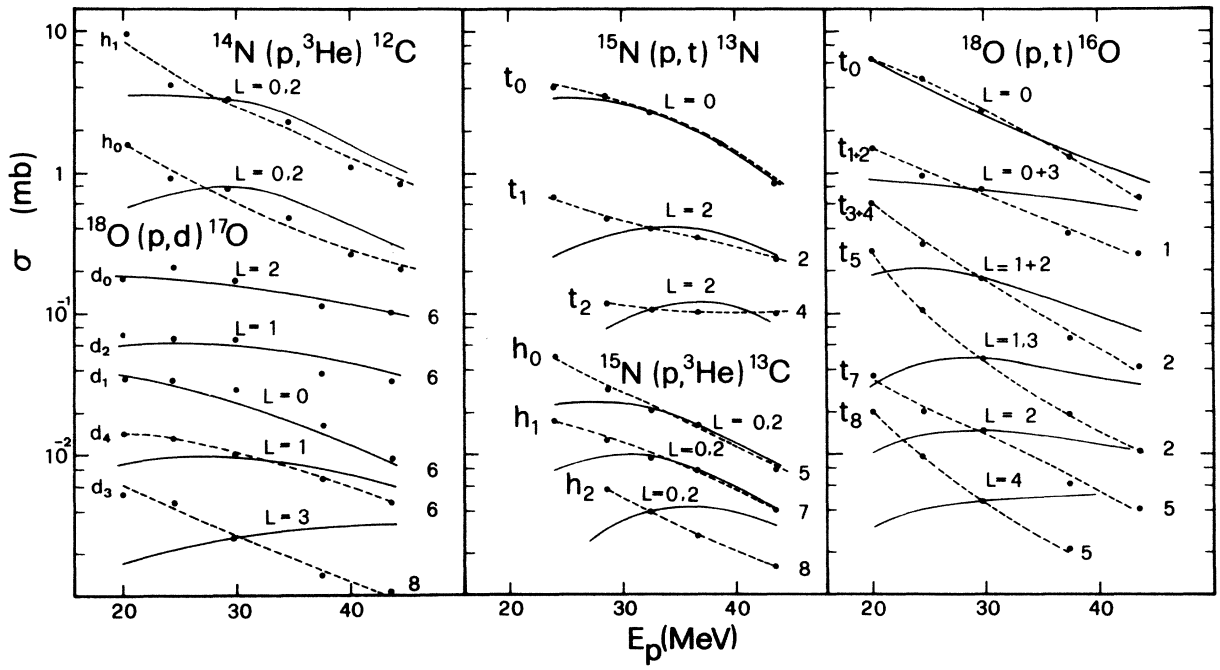

FIG. 11. Energy dependence of integrated cross sections. See Tables I–IV for details of the transitions. The curves represent the single-step DWBA energy dependence of the cross sections and are arbitrarily normalized to the data. The comma between two values of the transferred angular momentum L indicates coherent sum; the addition sign indicates incoherent sum. See caption for Fig. 1 for the numbers at the right hand side of the curves.

havior cannot be attributed to a particular choice of parameters not satisfactorily known as those of mass-3 optical model potentials. The presence of this maximum, not found in our experimental data, might suggest that DWBA method loses its validity outside the region in which matching conditions are verified or that other reaction mechanisms contribute substantially to the cross section.

Different kinematical conditions are encountered in the case of the energy dependence of the ^{18}O-$(p, d)^{17}O$ reaction. In this case the proton transmission coefficients are closer to those for deuterons than to those for mass-3 particles. It is therefore possible to have, at the same time, satisfactory matching conditions over a larger range of Q, L, and energy values than in a (p, t) or a $(p, {}^3He)$ reaction. A satisfactory over-all agreement is in fact found for this reaction, as one can observe in Fig. 11. The fits obtained for the ground state and the first two excited states, i.e., for strong allowed transitions, are very good. The calculations relative to the transition d_3 and, less markedly, to d_4 do not reproduce the experimental energy dependence. The first transition, leading to the $\frac{5}{2}^-$ state at 3.84 MeV in ^{17}O, should however contain large multi-step contributions. In fact a direct neutron pickup would require a sizeable $1f_{5/2}$ component in the ^{18}O ground state. In the case of the d_4 transition to the $\frac{3}{2}^-$ state at 4.55 MeV, single-step pickup mechanism contributions to the cross section have been found in a recent experiment.[36] The irregular behavior of the differential cross section with incident energy indicates however, the presence of also other mechanisms.

E. Spectroscopic amplitudes

It is an interesting result of this work that, as one can observe in Figs. 10 and 11, the ratio $\sigma_{exp}/\sigma_{DWBA}$ which is evaluated in order to extract spectroscopic information, may change even by one order of magnitude in the energy range 20–45 MeV. Most (p, t) and $(p, {}^3He)$ measurements on light nuclei have been performed at proton energies between 40 and 50 MeV. If one assumes that the best DWBA predictions are obtained at the energy at which the angular momentum matching conditions are verified, the σ_{DWBA} calculated in the 40–50 MeV energy range can be overevaluated by

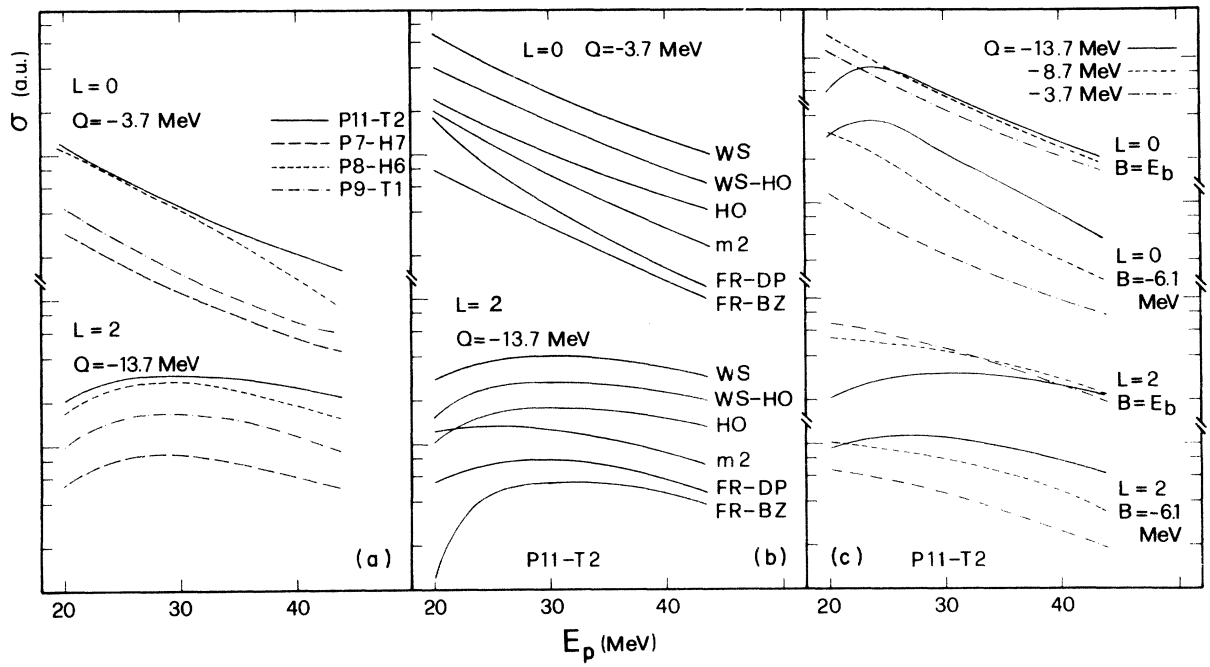

FIG. 12. Tests of the dependence on the various parameters of the single-step DWBA excitation function for two transitions of the $^{18}O(p, t)^{16}O$ reaction. (a) The effect on the calculated curves produced by the use of different optical model parameters (see Tables V and VI). (b) The dependence of DWBA results on the assumptions made to calculate the form factor and on finite range corrections: WS, Woods-Saxon wave functions; HO, harmonic oscillator wave functions; WS-HO, Woods-Saxon wave functions expanded in terms of harmonic oscillator wave functions; $m2$, transferred pair treated as a single mass-2 particle; FR-DP finite range calculation of Perrenoud and Devries (Ref. 35); FR-BZ finite range correction of Bencze and Zimanyi (Ref. 31). (c) The effect of changing the Q value and binding energy B of the transferred particle: $E_B = \frac{1}{2}(S_{nn} + E_{exc})$ (see text). $E_B = 6.1$ MeV corresponds to $Q = -3.7$ MeV and $E_{exc} = 0$.

a large factor. The DWBA must, therefore, be handled very carefully in extracting spectroscopic information. As an example we shall discuss a recently published survey of (p,t) reactions on $1p$-shell nuclei.[2] In this work Kahana and Kurath have found that the experimental ratio between the cross sections for strong $L=0$ and $L=2$ transitions is larger by a factor of 2 than the calculated one. This discrepancy may, at least partly, be due to the fact that at the incident energy of 43.7 MeV, considered by these authors, the $L=2$ transitions are overevaluated by the DWBA. In fact if we take for the ratio t_0/t_2 in the $^{15}N(p,t)^{13}N$ reaction, the cross sections integrated between 15 and 50°, as done in Ref. 2, we find that at an incident energy of 28.6 MeV, for which matching conditions are approximately verified, the experimental and predicted ratios are, respectively, 2.63 and 2.94. They are therefore much more similar than those considered by the above authors at 43.5 MeV, which are 1.05 and 0.51, respectively.

Only few two-nucleon transfer experiments have been performed at several incident energies. Cosper *et al.*[11] have studied the energy dependence of the (p,t) reaction on ^{26}Mg and ^{12}C. Maxima are in this case found not only in the calculated excitation function but also in the experimental data; a good agreement is therefore obtained. Recently the (p,t) reaction at three incident energies on ^{22}Ne has been studied by Falk, Kulisic, and McDonald[3] who find that over the range from 26.9 to 42.9 MeV, the ratio $\sigma_{exp}/\sigma_{DWBA}$ is slightly increasing for $L=0$ transitions, while it is decreasing slightly for $L=2$ and strongly for $L=4$ transitions. This is the same effect found in the present work.

A similar situation occurs also in (p,d) reactions for very high negative Q values, like the $^{16}O(p,d)^{15}O$ reaction studied by Snelgrove and Kashy.[9] The spectroscopic factors deduced by these authors for two $L=1$ transitions ($Q=-13.44$ and -19.62 MeV) decrease from 3.2 to 1.8 and from 8.1 to 2.6, respectively, when the proton energy increases from 25.52 to 45.34 MeV.

IV. TWO-STEP PROCESSES

The shape of the calculated excitation functions of (p,t) and $(p,{}^3He)$ reactions depends strongly, as shown in Sec. III D, on the angular momentum matching conditions. This dependence results from the assumptions of the direct, single-step pickup model. Different excitation functions may be obtained if the reaction is considered to proceed through more complex mechanisms, such as two- or multi-step processes.

The marked diffraction pattern which characterizes the differential cross sections here reported excludes sizeable contributions of mechanisms involving a large number of degrees of freedom,

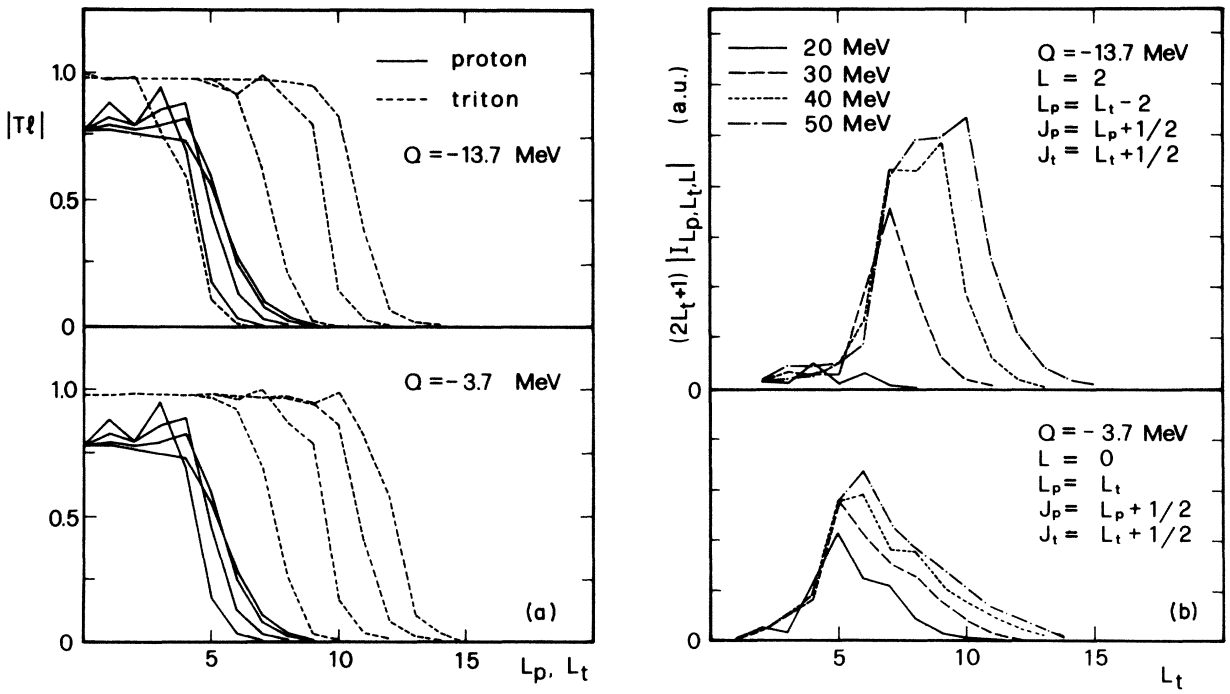

FIG. 13. (a) Typical transmission coefficients at four incident proton energies [given in (b)] and corresponding triton energies. Energies increase from left to right. (b) Moduli of the radial integrals.

such as the compound nucleus, and suggests consideration first of two-step processes.

Two-step processes of considerably large strength have been recently hypothesized in a variety of reactions.[12-14,37-46] The inclusion of a two-step reaction channel produces generally an energy dependence steeper than that of a single-step direct process[40,41] and therefore capable of a better agreement with the experimental data. The maximum in the excitation functions found using the single-step DWBA formalism may however still be present in the coupled channels calculations, as in those by Rawitscher[40] and might indicate that, at least in some cases, angular momentum matching conditions are still operating.

Inelastic coupled channels have been explicitly considered for two-nucleon transfer reactions by Asciutto and Glendenning[13] and by Tamura *et al.*[14] Recently, Olsen *et al.*,[45] in their coupled channels analysis of the ^{22}Ne$(p, t)^{20}$Ne data of Falk, Kulisic, and McDonald,[3] have obtained a satisfactory description of the cross section energy dependence for transitions leading to the ground state rotational band of ^{20}Ne.

For the nuclei here considered, which are not strongly deformed, other two-step mechanisms, like the successive single-nucleon pickup described by Kunz and Rost,[12] might instead become important. In this case the evaluation of the relative importance of the two-step processes may be critical, as stressed by Coker, Udagawa, and Wolter,[38] owing to the theoretical ambiguities inherent to the present stage of the calculations for both the direct and the successive pickup.

In this connection some physical criteria have been suggested.[43,46] Successive capture of nucleons can also be described by a quadrangular Feynman diagram. Recently these graphs have been considered also in connection with two-particle transfer reactions.[41-43] In particular Bang *et al.*[43] suggested that the difference $\Delta E = E_1 - E_2$ in the binding energy of the two successively transferred nucleons can be used as a physical criterion for the choice of contributing graphs. The two-nucleon pickup reaction from nucleus $A+2$ to the nucleus A proceeds through states of the $A+1$ nucleus

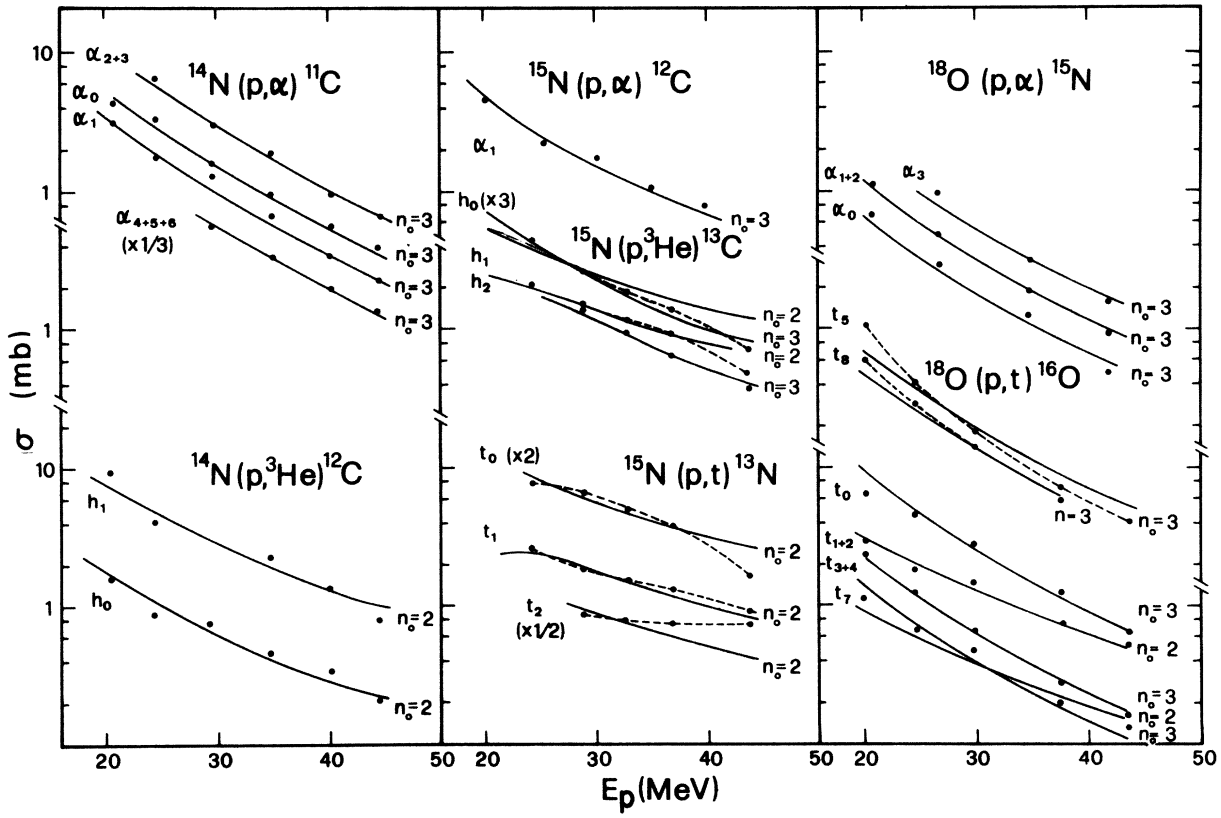

FIG. 14. Comparison of the experimental energy dependence (points and dashed curves) with the predictions of the preequilibrium model (see text). Triton and ^{3}He transitions are labeled as in Tables I–III; (p, α) transitions are as follows: to ^{11}C levels: α_0=ground state, α_1=1.99 MeV, α_2=4.3 MeV, α_3=4.79 MeV; to ^{12}C levels: α_1=4.43 MeV; to ^{15}N levels: α_0= ground state, α_1=5.27 MeV, α_2=5.30 MeV, α_3=6.32 MeV. The quantity n_0 is a parameter of the model (see text).

which are connected by fractional parentage coefficients to both A and $A+2$ nuclei. When $\Delta E \gtrsim 30$ MeV the four point graph, corresponding to the successive independent capture of the two nucleons, should dominate. In our cases ΔE values have been evaluated using the coefficients of fractional parentage given by Cohen and Kurath[21] for ^{14,15}N and by Zuker[22] for ^{18}O. The resulting values are smaller than 20 MeV for all the transitions relative to the reactions on ^{18}O and ^{14}N and smaller than 10 MeV for those on ^{15}N.

Another criterion suggested by Wolter, Udagawa, and Olsen[46] for transitions to unnatural parity states, which are forbidden in a single-step mechanism, can be applied to the (p, t) transition leading to the 2^- state at 8.88 MeV in ^{16}O. According to this criterion the differential cross section goes to zero at forward angles for a two-step process via the inelastic channel, whereas it remains finite for successive pickup. In the present case no clear indication can be derived also because the shape of the angular distribution at small angles changes with incident energy, as shown in Fig. 3.

Even if the suggested physical criteria do not give *a priori* a clear indication of substantial contributions from two-step pickup, we believe that a detailed calculation would be highly desirable for the reactions here studied for the reasons given above.

Finally it should be remarked that if the disagreement between the calculated and the experimental excitation functions is taken as an indication of the importance of two-step contributions, a large contribution would be required also for high intensity transitions, such as that leading to the doublet at 6.1 MeV in ^{16}O, which is labeled as t_{1+2} in Fig. 11, or those to the excited states in ^{12}C and ^{13}C.

V. PREEQUILIBRIUM MODEL

The preequilibrium emission model has recently been applied successfully to interpret certain aspects of nuclear reactions which seem to require a limited number of steps and therefore cannot be explained in the framework of the direct interaction or of the compound nucleus model.

Recently it has been shown[17,47] that the energy dependence of (p, α) reactions in light nuclei can be reproduced. The energy dependence of the cross section for a reaction from the initial channel α to the final channel β can be expressed as[48]:

$$\sigma_{\alpha,\beta} \cong \sigma_R(\alpha) \frac{W_c^{n_0}}{W_c^{n_0} + W_{eq}^{n_0}} \frac{W_{c\beta}^{n_0}}{W_c^n} . \qquad (2)$$

$\sigma_R(\alpha)$ is the reaction cross section for the incident particle, W_c^n the decay probability per unit time into the continuum via one particle emission from an n_0 exciton state, $W_{c\beta}^n$ the emission probability per unit time into channel β, and W_{eq}^n the probability per unit time for the n_0 state to evolve towards the equilibrium configuration. This last quantity has been evaluated according to Williams[49] with W_{eq}^1 as given by Birattari *et al.*[48] for a Fermi energy equal to 40 MeV.

The level density of single particle states entering in the calculation of $W_c^{n_0}$ has been taken as in the previous work.[17] The inverse cross sections have been calculated using the optical model parameters of set $P2$ for protons, of Becchetti and Greenless[50] for neutrons, of set $H4$ for tritons and helium-3, and the parameters given by Hird and Li[51] for α particles.

The resulting excitation functions are reported in Fig. 14. A satisfactory agreement with the slope of the (p, α) excitation functions is again[17] obtained with a value of $n_0 = 3$.

In this simple model the structure of the involved states is not taken into account. The energy dependence is essentially governed by the preequilibrium deexcitation of the first intermediate state via nucleon emission. One would therefore expect the same qualitative behavior for the excitation functions of different reactions on the same nucleus. On the contrary the (p, t) and $(p, ^3\text{He})$ reaction energy dependence cannot generally be fitted with the n_0 value obtained from the (p, α) reactions, but often requires a lower value as in the case of ^{14}N. Moreover, as clearly shown by the ^{18}O(p, t)-^{16}O reaction, different transitions require different n_0 values. Finally the ^{15}N$(p, t_2)^{13}$N transition cannot be fitted by the model. These variations of the value of n_0 for different reactions or for different transitions in the same reaction on a given nucleus pose intrinsic difficulties and probably evidence the fact that other mechanisms more dependent on the structure of the involved states are important.

VI. CONCLUDING REMARKS

The (p, t) and $(p, ^3\text{He})$ reactions here studied present uniformly decreasing cross sections in the incident energy range between 20 and 45 MeV. This energy dependence cannot be explained by standard DWBA calculations based on a single-step, two-nucleon pickup. When such an analysis is attempted effects connected with the existence of angular momentum matching conditions are evidenced. These conditions can, in fact, be met only in a limited range of incident energies which is centered around a value depending upon the angular momentum transfer and the Q value of the transition considered. When this energy value lies

within the measured interval, a broad maximum, not found in the experiment, is present in the calculated excitation function.

This result may reflect the fact that the DWBA method gives reliable results only in the energy region in which matching conditions are verified or be indicative of substantial contributions from other reaction channels corresponding to two- or multi-step processes. Both effects could also be present at the same time.

Multi-step calculations based on the pre-compound model, given in Sec. V, raise doubts on the reliability of the model when applied to the above reactions.

We cannot at this stage draw definite conclusions about successive single-nucleon transfer mechanisms since detailed calculations including these processes have not been performed; we feel however that the present experimental data constitute an useful test for future two-step analysis of two-nucleon transfer reactions.

The authors are grateful to Professor J. M. Nelson for having kindly supplied the Oxford code for two-nucleon transfer reactions and to Dr. R. M. Devries for finite-range calculations.

[1]N. K. Glendenning, Phys. Rev. 137, B102 (1965).
[2]S. Kahana and D. Kurath, Phys. Rev. C 3, 543 (1971).
[3]W. R. Falk, P. Kulisic, and A. McDonald, Nucl. Phys. A167, 157 (1971).
[4]D. G. Fleming, J. Cerny, C. C. Maples, and N. K. Glendenning, Phys. Rev. 166, 1012 (1968).
[5]R. A. Paddock, Phys. Rev. C 5, 485 (1972).
[6]R. Stock, R. Bock, P. David, H. H. Duhm, and T. Tamura, Nucl. Phys. A104, 136 (1967).
[7]L. L. Lee, Jr., J. P. Schiffer, B. Zeidman, G. R. Satchler, R. M. Drisco, and R. H. Bassel, Phys. Rev. 136, B971 (1964).
[8]M. B. Hooper, Nucl. Phys. 76, 449 (1966); B. Buck and J. R. Rook, Nucl. Phys. 67, 504 (1965).
[9]J. L. Snelgrove and E. Kashy, Phys. Rev. 187, 1246 (1969).
[10]N. Austern, *Direct Nuclear Reaction Theories* (Wiley, New York, 1970), Chap. V.
[11]S. W. Cosper, H. Brunnader, J. Cerny, and L. McGrath, Phys. Lett. 25B, 324 (1967).
[12]P. D. Kunz and E. Rost, University of Colorado Technical Progress Report No. COO-535-674, 1972 (unpublished).
[13]R. J. Ascuitto and N. K. Glendenning, Phys. Rev. C 2, 415, 1260 (1970).
[14]T. Tamura, D. R. Bes, R. A. Broglia, and S. Landowne, Phys. Rev. Lett. 25, 1507 (1970).
[15]J. J. Griffin, Phys. Rev. Lett. 17, 478 (1966); Phys. Lett. 24B, 5 (1967).
[16]M. Blann, Phys. Rev. Lett. 21, 1357 (1968).
[17]P. Guazzoni, I. Iori, S. Micheletti, N. Molho, M. Pignanelli, and G. Semenescu, Phys. Rev. C 4, 1092 (1971).
[18]I. S. Towner and J. C. Hardy, Advan. Phys. 18, 401 (1969).
[19]P. D. Kunz, code DWUCK, private communication; J. M. Nelson and B. E. F. Macefield, Oxford Nuclear Physics Laboratory Report No. 18/69 (unpublished).
[20]J. M. Nelson, N. S. Chant, and P. S. Fisher, Nucl. Phys. A156, 406 (1970).
[21]S. Cohen and D. Kurath, Nucl. Phys. A141, 145 (1970).
[22]A. P. Zuker, B. Buck, and J. B. McGrory, Phys. Rev. Lett. 21, 39 (1968); A. P. Zuker, Phys. Rev. Lett. 23, 983 (1968) and private communication.
[23]M. A. Melkanoff, J. Raynal, and T. Sawada, MERCY code, UCLA Report No. UCLA 66-10, 1966 (unpublished).
[24]B. A. Watson, P. P. Singh, and R. E. Segel, Phys. Rev. 182, 977 (1969).
[25]J. J. H. Menet, E. E. Gross, J. J. Malinify, and A. Zucker, Phys. Rev. C 4, 1114 (1971).
[26]R. N. Glover and A. D. W. Jones, Phys. Lett. 16, 69 (1965).
[27]L. R. Scherk and W. R. Falk, Nucl. Phys. A183, 240 (1972).
[28]R. M. Del Vecchio and W. W. Daehnick, Phys. Rev. C 6, 2095 (1972).
[29]J. C. Hiebert, E. Newman, and R. H. Bassel, Phys. Rev. 154, 898 (1967).
[30]W. T. H. Van Oers and J. M. Cameron, Phys. Rev. 184, 1061 (1969).
[31]G. Bencze and J. Zimanyi, Nucl. Phys. 81, 76 (1966).
[32]J. Joseph, C. Fayard, E. El-Baz, and J. Lafoucrière, Nucl. Phys. A142, 217 (1970).
[33]N. S. Chant and N. F. Mangelson, Nucl. Phys. A140, 81 (1970).
[34]J. L. Perrenoud and R. M. Devries, Phys. Lett. 36B, 18 (1971).
[35]R. M. Devries, private communication.
[36]M. Pignanelli, J. Gosset, F. Resmini, B. Mayer, and J. L. Escudié, Phys. Rev. C 8, 2120 (1973).
[37]M. Toyama, Phys. Lett. 38B, 147 (1972).
[38]W. R. Coker, T. Udagawa, and H. H. Wolter, Phys. Rev. C 7, 1154 (1972).
[39]R. Ascuitto, N. K. Glendenning, and B. Sørensen, Nucl. Phys. A170, 65 (1971).
[40]G. H. Rawitscher, Phys. Rev. 163, 1223 (1967).
[41]E. Zh. Magzumov, V. G. Neudachin, and M. S. Belkin, Yad. Fiz. 11, 589 (1970) [transl.: Sov. J. Nucl. Phys. 11, 331 (1970)].
[42]V. Vanzani, Lett. Nuovo Cimento 3, 399 (1970).
[43]J. Bang, N. S. Zelenskaya, E. Zh. Magzumov, and V. G. Neudachin, Yad. Fiz. 4, 962 (1966) [transl.: Sov. J. Nucl. Phys. 4, 688 (1967)].
[44]T. Udagawa, T. Tamura, and T. Izumuto, Phys. Lett. 35B, 129 (1971).
[45]D. K. Olsen, T. Udagawa, T. Tamura, and R. E. Brown, in *Proceedings of the International Conference on Nuclear Physics, Munich, 1973*, edited by J. de Boer and H. J. Mang (North-Holland, Amsterdam/American Elsevier, New York, 1973), Vol. I, p. 489.
[46]H. H. Wolter, T. Udagawa, and D. K. Olsen, in *Proceedings of the International Conference on Nuclear Physics, Munich, 1973* (see Ref. 45), Vol. I, p. 492.

[47]E. Gadioli, Lett. Nuovo Cimento 3, 515 (1972).
[48]C. Birattari, E. Gadioli, E. Gadioli Erba, A. M. Grassi Strini, G. Strini, and G. Tagliaferri, Nucl. Phys. A201, 579 (1973).
[49]F. C. Williams, Jr., Phys. Lett. 31B, 184 (1970).
[50]F. D. Becchetti and G. W. Greenlees, Phys. Rev. 182, 1190 (1969).
[51]B. Hird, and T. Y. Li, Can. J. Phys. 46, 1273 (1968).